Synthesis and dielectric properties of barium tantalates and niobates with complex perovskite structure

T. Kolodiazhnyi and A. Petric[a)]
Department of Materials Science & Engineering, McMaster University, Hamilton, ON, L8S 4L7, Canada

A. Belous, O. V'yunov, and O. Yanchevskij
Department of Solid State Chemistry, Institute of General and Inorganic Chemistry, 32/43 Palladina Ave., Kyiv-142, Ukraine

(Received 31 July 2002; accepted 19 September 2002)

Phase composition, degree of cation ordering, and dielectric properties of complex perovskites with general formula $Ba(B'_{1/3}B''_{2/3})O_3$, where B′ = Mg, Zn, and Ni and B″ = Nb and Ta, were analyzed. It was found that all the studied complex perovskites attained high degrees of 1:2 cation ordering at temperatures specific to each composition. A high temperature order–disorder phase transition in $Ba(Zn_{1/3}Nb_{2/3})O_3$ occurred below 1380 °C. $Ba(Ni_{1/3}Nb_{2/3})O_3$ (BNN) and $Ba(Mg_{1/3}Nb_{2/3})O_3$ (BMN) pervoskites remained 100% ordered at temperatures as high as 1500 and 1620 °C, respectively. It was found that in BMN and BNN extrinsic factors, such as the second phase (i.e., $Ba_3Nb_5O_{15}$) and point defects, dominated the dielectric loss at microwave frequencies. $Ba(Mg_{1/3}Ta_{2/3})O_3$ (BMT) remained single phase up to 1630 °C. Above this temperature, the $Ba_3Ta_5O_{15}$ second phase was detected. A decrease in the 1:2 cation ordering and increase of dielectric loss in BMT occurred at sintering temperatures above 1590 °C. It was also revealed by electron paramagnetic resonance that all samples studied contained a substantial amount of paramagnetic point defects. These defects contributed to extrinsic dielectric loss at microwave frequencies, thus degrading the *Q* factor.

I. INTRODUCTION

Low-loss temperature-stable dielectric resonators are used extensively as input and output multiplexers in communication satellites, band-stop and band-pass filters, feedback circuits for microwave oscillators, etc.[1] Recent breakthroughs in the design of dielectric resonators shielded with high-temperature superconductor walls show promise in fulfilling new requirements for future communication systems.[2] Complex perovskites with the general formula $Ba(B'_{1/3}\ B''_{2/3})O_3$, where B′ = Mg and Zn and B″ = Ta, have proved to be the most suitable candidates for application in X, K_u, and K frequency bands (i.e., 8–27 GHz). They satisfy three important requirements imposed on microwave dielectrics, i.e., high dielectric constant ($\epsilon \approx 24$–30), high $Q \times f$ value ($Q \times f \approx 100$–300 THz, where *Q* is the quality factor and *f* is the resonance frequency), and near-zero temperature coefficient of the resonance frequency, τ_f. Tremendous research efforts were undertaken to improve the properties[3,4] as well as to understand the dominant mechanism of the dielectric loss in these materials.[5,6]

Intrinsic microwave dielectric loss in $Ba(B'_{1/3}B''_{2/3})O_3$ originates from the two-phonon difference absorption process.[7] The only way to minimize this loss is to achieve a complete 1:2 ordering of B′ and B″ cations. However, recent studies suggest that extrinsic dielectric loss due to the point defects or second phase may dominate in practical ceramics.[6,8] The presence of the point defects (e.g., vacancies, dopant ions) may alter the phonon spectrum resulting in a one-phonon absorption mechanism at microwave frequencies. For example, the problem of stabilization of the oxidation state of Ni in $Ba(Zn_{1/3}Ta_{2/3})O_3$ ceramics doped with Ni and Zr has been recently addressed by Rong *et al.*[6]

Until now, most research efforts were restricted to the investigation of $Ba(Mg_{1/3}Ta_{2/3})O_3$ (BMT) and $Ba(Zn_{1/3}Ta_{2/3})O_3$, compounds owing to their wide commercial utilization.[6,9] It is useful to know whether other $Ba(B'_{1/3}B''_{2/3})O_3$ complex perovskites might show similar dependence of their dielectric properties on preparation conditions. Several complex perovskites including $Ba(Mg_{1/3}Ta_{2/3})O_3$, $Ba(Mg_{1/3}Nb_{2/3})O_3$ (BMN), $Ba(Ni_{1/3}Ta_{2/3})O_3$ (BNT), $Ba(Ni_{1/3}Nb_{2/3})O_3$ (BNN), and $Ba(Zn_{1/3}Nb_{2/3})O_3$ (BZN), further abbreviated as BMT, BMN, BNT, BNN, and BZN were chosen for this study. The information about their dielectric properties is

a)Address all correspondence to this author.
e-mail: petric@mcmaster.ca

somewhat inconsistent (see Table I). BZN, BNN, and $Ba(Co_{1.3}Nb_{2/3})O_3$ were initially considered disordered perovskites.[18–20] Later, Yoshioka[21] and Akbas and Davies[22] showed that BZN can be prepared with 1:2 cation ordering when sintered at 1350 °C. Hong *et al.*[23] and Molodetsky and Davies[24] reported that, below 1400 °C, BNN and $Ba(Co_{1/3}Nb_{2/3})O_3$ have an ordered 1:2 perovskite structure. The order–disorder temperature of $Ba(Zn_{1/3}Ta_{2/3})O_3$ reported by different authors varies from 1600 to 1625 °C.[25,26] One can also find a major discrepancy between experimental and theoretical values of the high-temperature order–disorder phase transition for $Ba(B'_{1/3}B''_{2/3})O_3$ compounds. Often measured temperatures of the order–disorder phase transition are ca. 1000 °C lower than calculated ones.[27,28]

This paper examines the effect of preparation conditions on the degree of cation ordering, phase composition, and dielectric properties of BMT, BMN, BZN, BNN, and BNT complex perovskites.

II. EXPERIMENTAL

BMT, BMN, BZN, BNN, and BNT powders were prepared by the solid-state method using $MgTa_2O_6$, $MgNb_2O_6$, $ZnNb_2O_6$, $NiNb_2O_6$, $NiTa_2O_6$, and $BaCO_3$ precursors. As was found in earlier studies,[29] this method offers several advantages over using simple metal oxide precursors. For example, it yields single-phase ceramics at lower sintering temperatures and also results in higher density and lower dielectric loss. Following ball milling in an alcohol slurry for 2 h, the milled powders were dried and then calcined at 900–1200 °C for 5 h. The calcined powders were reground and vibromilled for 10 h and then dried, mixed with poly(vinyl alcohol) binder, and pressed into pellets at 800 kg/cm^2 pressure. The pellets were sintered in air at temperatures of 1300–1650 °C for 20 h. Several BMT samples were also sintered at 1700 °C for 5 h. The heating and cooling rates were varied from 15 to 200 °C/h. Phase identification was performed on a Rigaku Geigerflex Dmax II (Rigaku, Tokyo, Japan) diffractometer with a Co K_α radiation source ($\lambda = 1.7889$ Å), a step size of 0.02°, and a count time of 4 s/step. The microstructure of polished samples was studied by scanning electron microscopy (Philips 515, Philips Electronic Instruments, Amsterdam, The Netherlands) equipped with energy dispersive spectroscopy (EDS); (Link Analytical, Bucks, United Kingdom).

TABLE I. Dielectric properties of several $Ba(B'_{1/3}B''_{2/3})O_3$ compounds.

System	ϵ	$Q \times f$ (THz)	τ_f (ppm/K)	Ref.
$Ba(Mg_{1/3}Ta_{2/3})O_3$	24	430	+5.4	[4]
	23–24	300	−2.0 to +2.0	[10]
	22.5–23.9	280	−0.3 to 3.5	This work
$Ba(Mg_{1/3}Nb_{2/3})O_3$	32	55	+33	[11]
	31–34	40	+21	[12]
	32	71	+30	[13]
	32	65	+18.8	[14]
	31.4	160	+14.2 to +34	This work
$Ba(Ni_{1/3}Ta_{2/3})O_3$	23	50	−18	[15]
	22	95.5	−10.5 to −13.5	This work
$Ba(Ni_{1/3}Nb_{2/3})O_3$	36	70	+20	[16]
	35.4	35	−4.9 to +5	This work
$Ba(Zn_{1/3}Nb_{2/3})O_3$	41	87	+31	[11]
	41	55	+31	[17]
	40	69	+20.7 to +23	This work

Electron paramagnetic resonance (EPR) studies were performed at 25 °C. A Bruker EMX 8/2.7 (Bruker Instruments, Inc., Billerica, MA) X-band EPR spectrometer was used. Ceramic samples were ground into powders. The weight of the powdered samples was kept at 50 ± 1 mg. Measurements were performed in the frequency range 9.4–9.8 GHz and at a constant microwave power of 2 mW. Analysis of the resonance spectra was conducted with WIN-EPR software (Bruker Instruments, Inc., Billerica, MA).

Dielectric characterization of the samples in the X-frequency band was performed with an HP 8510 (Hewlett Packard, Santa Rosa, CA) vector network analyzer using the transmission waveguide method. For transmission measurements, a cylindrical dielectric resonator (DR) shaped into a $TE_{01\delta}$ resonant mode was centered in the X-band rectangular copper waveguide using a styrofoam holder. In this configuration, the waveguide serves as a band-stop filter at the $TE_{01\delta}$ resonance frequency. To separate the $TE_{01\delta}$ mode from the higher resonance modes, the samples must have an aspect ratio close to 0.45. The diameter and thickness of the samples were 6 and 2.7 mm, respectively. The unloaded Q factor was calculated according to

$$Q = \frac{Q_L}{1 - 10^{-P/20}} \quad , \tag{1}$$

where Q_L is the loaded quality factor determined from the full width of the resonance peak at the 3 dB level and P is the depth of the resonance peak in decibels. The accuracy of the transmission method setup has been tested by using two commercially available dielectric resonators, Murata (Murata DRD065FD029A, $Q = 30000$, $f_c = 9.98$ GHz, $\epsilon' = 24 \pm 1$, $\tau_f = 2 \pm 1$ ppm/K) F-series DR and OXIDE (OXIDE, $BaTi_4O_9$, $Q = 6000$, $f_c = 9.6$ GHz, $\epsilon' = 36 \pm 0.5$, $\tau_f = 0 \pm 0.3$ ppm/K) barium tetratitanate DR. The results showed that the Q factor agreed to 0.1% of that specified and that f_c was higher by 2% and 0.5% for Murata and OXIDE DRs, respectively. The real part of the dielectric constant, ϵ', in the X-band was calculated according to[30]

$$\epsilon' \approx \left[\frac{34}{r f_c}\left(\frac{r}{d} + 3.45\right)\right]^2 \quad , \tag{2}$$

where r is the radius of the DR, d is the thickness of the DR, and f_c is the resonant frequency in GHz. Strictly speaking, Eq. (2) is applicable for $30 < \epsilon' < 50$, and

it underestimates ϵ' by 5–7% for materials with $20 < \epsilon' < 30$. Temperature dependence of the resonance frequency was measured in the range of +20 to +90 °C. For measurement of τ_f, the sample was placed in a porous, low-ϵ' ceramic holder with a small thermal expansion coefficient. The waveguide was wrapped with a resistive heating tape, and the temperature was monitored using a K-type thermocouple attached to the outer surface of the waveguide. The temperature coefficient of the resonant frequency is defined by

$$\tau_f = \frac{\Delta f_c}{f_c \Delta T} \quad , \tag{3}$$

where Δf_c is the shift of the resonant frequency, f_c, introduced by the temperature change ΔT.

III. RESULTS AND DISCUSSION

A. Phase composition

Within the x-ray diffraction (XRD) accuracy of ca. 2%, BMT, BMN, BNT, BNN, and BZN powders formed single-phase perovskite compounds at 1100, 1000, 950, 1000, and 950 °C, respectively. No undesirable satellite secondary phases were detected during calcination. This is in contrast to the conventional synthesis method, which results in several undesirable second phases (e.g., $Ba_4Ta_2O_9$, $Ba_5Ta_4O_{15}$ in the case of BMT).[29,31,32] Hence, it can be concluded that the synthesis method employed in this work gives single-phase complex perovskites formed according to the following reaction:

$$B'B''_2O_6 + BaO \rightarrow Ba(B'_{1/3}B''_{2/3})O_3 \quad . \tag{4}$$

As revealed by XRD analysis, up to a critical temperature, BMT, BMN, BZN, and BNN compounds remained single phase. However, above a critical temperature, which is unique to each compound (see Table II), a small amount of second phase appeared. In BMT sintered above 1630 °C, the second phase was identified as $Ba_3Ta_5O_{15}$.[33] The $Ba_3Nb_5O_{15}$ phase[34] was detected in BMN and BNN compounds sintered at 1550 and 1500 °C, respectively. We were unable to identify the second phase in the BZN compound sintered above 1450 °C. It is quite possible that the XRD pattern comprises several different phases. As a result, the effect of the second phase on dielectric properties of BZN was different from that of BMN and BNN. Only the BNT compound remained single phase up to the maximum sintering temperature of 1610 °C. The XRD patterns of BMT, BMN, BNN, and BZN single-phase compounds as well as compounds containing the high-temperature second phase are shown in Fig. 1.

TABLE II. The second phase and the temperature of its formation in the compounds studied.

Compound	Second phase	T (°C)
BMT	$Ba_3Ta_5O_{15}$	1630
BMN	$Ba_3Nb_5O_{15}$	1550
BNT	…	…
BNN	$Ba_3Nb_5O_{15}$	1500
BZN	Unidentified	1460

B. 1:2 Cation ordering

$Ba(B'_{1/3}B''_{2/3})O_3$ perovskites can exist in disordered or 1:2 ordered phases. The ability of $Ba(B'_{1/3}B''_{2/3})O_3$ to order depends on the size, valence, and mass of the B-site cations. The degree of 1:2 ordering also depends on the sample preparation. From a crystallographic point of view, the ordering parameter S can be defined by the difference between on-site and off-site ions occupying B′ and B″ sites:

$$S = B''_{B''} - B''_{B'} = B'_{B'} - B'_{B''} \quad , \tag{5}$$

where $B''_{B''}$ is the fraction of B'' ions in B'' sites, $B''_{B'}$, is the fraction of B' ions in B'' sites, and so on. The ordering parameter can be deduced from the ratio of the x-ray intensities of the diffraction peaks associated with cation ordering. In $Ba(B'_{1/3}B''_{2/3})O_3$ perovskites, the ordering parameter, S, is determined by the ratio of the intensity of

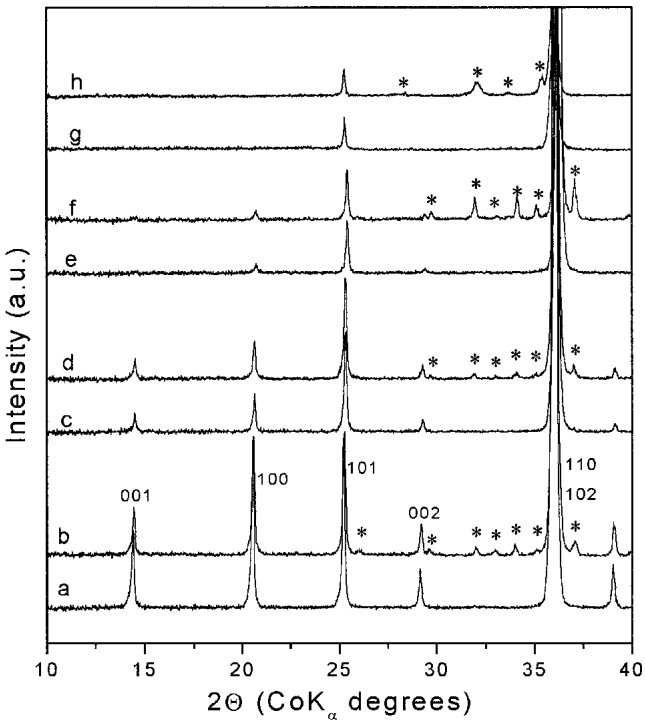

FIG. 1. XRD pattern of (a) BMT–1580 °C, (b) BMT–1700 °C, (c) BMN-1450 °C, (d) BMN–1620 °C, (e) BNN–1380 °C, (f) BNN–1500 °C, (g) BZN–1380 °C, and (h) BZN–1460 °C. Reflections from the second phase are indicated by an asterisk.

the strongest supperlattice reflection, (100), to the strongest peak of the $Ba(B'_{1/3}B''_{2/3})O_3$ structure, (110). Since the (012) and (102) peaks are very close to (110) they also should be taken into account in the calculations. Thus, ordering parameter is given by

$$S = \sqrt{\frac{(I_{100}/I_{110,012,102})_{obs}}{(I_{100}/I_{110,012,102})_{calc}}} \quad , \qquad (6)$$

where $(I_{100}/I_{110,012,102})_{obs}$ is the ratio of the observed intensity of the (100) superlattice reflection to that of (110,012,102) main reflection, and $(I_{100}/I_{110,012,102})_{calc}$ is the calculated value for a completely ordered structure. The values of $I_{100}/I_{110,012,102}$ for several $Ba(B'_{1/3}B''_{2/3})O_3$ compounds having completely ordered 1:2 structure calculated for Cu K_α and Co K_α x-ray radiation sources are listed in Table III. These values were used to determine the degree of 1:2 cation ordering in samples studied in this work.

Dependence of the ordering parameter, *S*, on calcining or sintering temperature for BMT, BMN, BNT, BNN, and BZN samples is shown in Fig. 2. For BMT, the value of *S* increases with sintering temperature, goes through a maximum of 0.995 at 1580 °C, and then decreases to 0.91 at 1700 °C. An important result is that the ordering parameter of the sample sintered at 1700 °C did not increase after postsinter anneal at 1580 °C for 20 h.

In BMN samples, the complete ordering was achieved upon treatment at 1620 °C. The BNT samples showed a maximum degree of ordering of 95% after sintering at 1610 °C. The BZN samples were completely ordered at 1200 °C. However, at 1380 °C and above, the BZN forms a disordered cubic perovskite phase in agreement with the results of Yoshioka[21] and Hong *et al.*[23] The ordering behavior of the BNN sample in this study was quite different from that reported by Hong *et al.*[23] Although in both cases it showed a high degree of 1:2 ordering, in this study, the BNN sample remained ordered up to 1500 °C, whereas, in the work of Hong *et al.*,[23] the BNN sample underwent an order–disorder phase transition above 1350 °C. This suggests that the mechanism of disordering in BNN depends not only on thermodynamic factors but also on the preparation history of the sample.

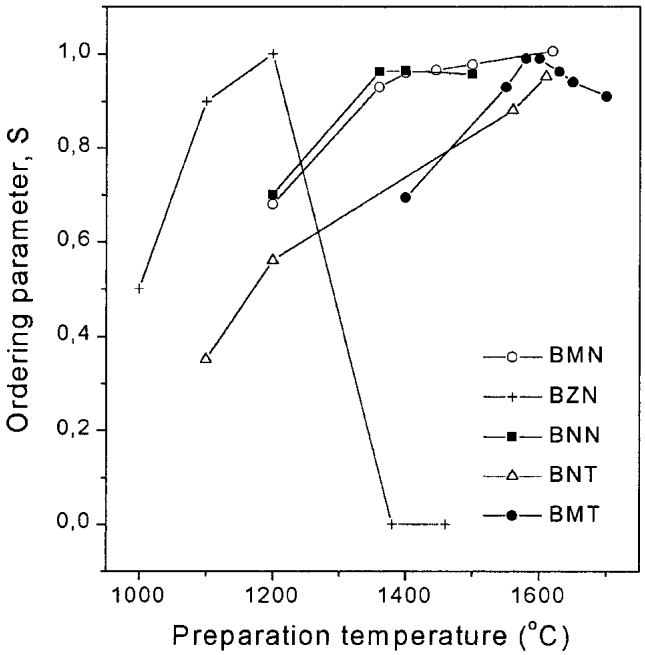

FIG. 2. Ordering parameter for BMT, BMN, BZN, BNN, and BNT samples calcined or sintered at different temperatures.

C. Density and microstructure

A number of investigations indicated that both the low dielectric loss and high dielectric constant could be only realized in ceramics having a relative density of higher than ca. 94%.[35–38] Figure 3 shows the dependence of the ceramic density on sintering temperature. The density of BMT, BMN, BZN, and BNN samples increased with sintering temperature to a maximum and then gradually decreased at higher sintering temperature. The maximum relative densities obtained for BMT, BMN, BNN, and BZN samples were 97.3%, 99.1%, 96.3%, and 98.1%, respectively. The maximum density of BNT samples sintered at 1610 °C was 97.1%. The relative densities were calculated from

$$\rho = \frac{\rho_m}{\rho_{th}} \times 100\% \quad , \qquad (7)$$

TABLE III. Calculated values of structure factors and $I_{100}/I_{110,012,102}$ for several $Ba(B'_{1/3}B''_{2/3})O_3$ compounds with completely ordered 1:2 structure.

Compound	F_{100}	F_{110}	F_{102}	F_{012}	$I_{100}/I_{110,012,102}$ Cu K_α	$I_{100}/I_{110,012,102}$ Co K_α
$Ba(Mg_{1/3}Ta_{2/3})O_3$	−58.31	256.90	−54.43	257.01	0.0827	0.0842
$Ba(Ni_{1/3}Ta_{2/3})O_3$	−42.98	270.89	−40.43	271.01	0.0404	0.0412
$Ba(Zn_{1/3}Ta_{2/3})O_3$	−40.86	273.04	−38.28	273.16	0.0359	0.0366
$Ba(Mg_{1/3}Nb_{2/3})O_3$	−27.15	197.14	−24.54	197.24	0.0304	0.0310
$Ba(Ni_{1/3}Nb_{2/3})O_3$	−11.82	211.13	−10.54	211.24	0.00503	0.00512
$Ba(Zn_{1/3}Nb_{2/3})O_3$	−9.69	213.28	−8.40	213.39	0.00331	0.00337

where ρ_m is the measured density and ρ_{th} = 7.657, 6.236, 8.017, 6.554, and 6.511 g/cm^3 is the theoretical density of BMT, BMN, BNT, BNN, and BZN, respectively.[39]

Microstructural observations of the samples revealed a gradual increase of the grain size with sintering temperature as shown in Fig. 4. The average grain size of the BMT samples increased from 2.5 to 20 μm for ceramics sintered at 1570–1700 °C. A second phase is clearly visible in BMT samples sintered at 1700 °C (Fig. 5). EDS analysis revealed that the Ba/Ta ratio was 0.888 and 0.357 for the matrix and the second phase, respectively. The grain size of BMN ceramics increased from 3.5 to 7–8 μm for samples sintered at 1400–1620 °C. A second phase was visible in ceramics sintered at 1620 °C. This second phase was enriched with Nb and depleted of Mg. The BNN ceramic showed an increase in the grain size from 1.5 to 4.5 μm for samples sintered in the temperature interval from 1400 to 1500 °C. The grain size of BNT samples sintered at 1570–1610 °C was in the range 2.0–3.5 μm. A Ta-rich second phase was observed on the surface of thermally etched BNT samples. The grain size of BZN ceramics increased from 5 to 20 μm for ceramics sintered at 1380–1460 °C. The chemical composition of the BZN matrix and the second phase formed at the surface of the pellets was analyzed using EDS. It was found that the second phase was depleted of Zn ions, but the Ba/Nb ratio was the same as that of the matrix phase.

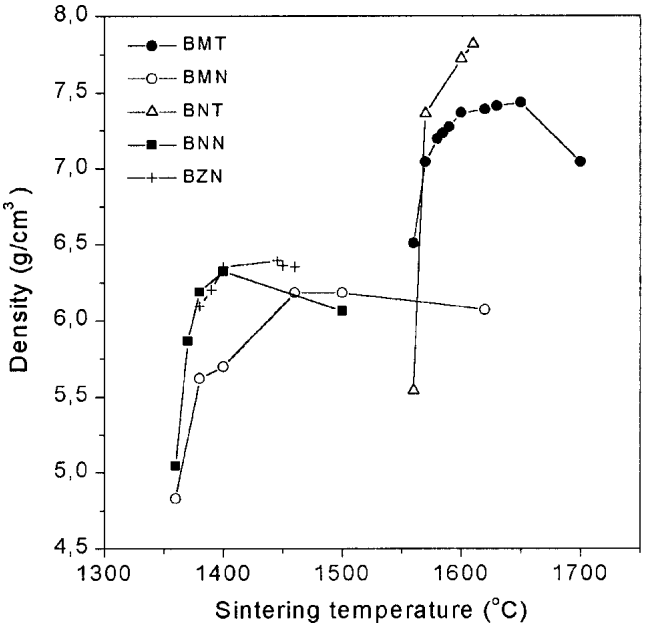

FIG. 3. Density of BMT, BMN, BZN, BNN, and BNT samples sintered at different temperatures.

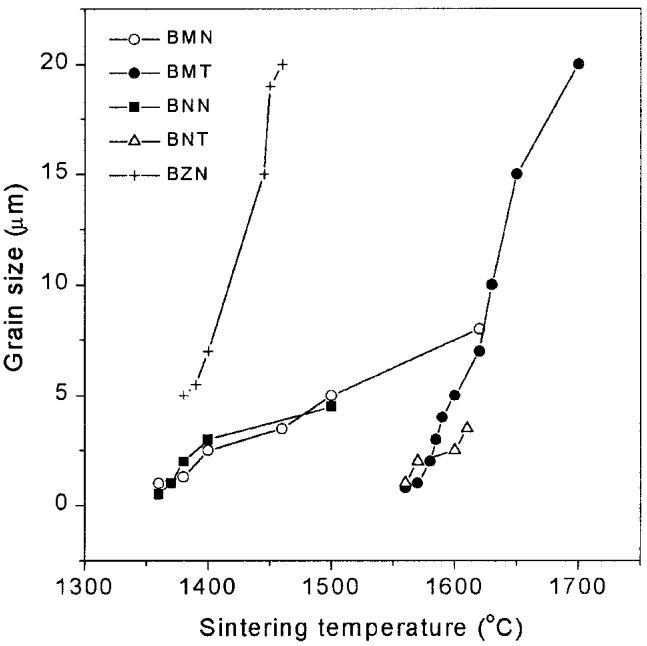

FIG. 4. Grain size of BMT, BMN, BZN, BNN, and BNT samples sintered at different temperatures.

D. Dielectric properties

The effect of the sintering temperature on the dielectric constant, ϵ', of BMT, BMN, BNT, BNN, and BZN ceramics is shown in Fig. 6. For BMN, BNN, and BNT samples, ϵ' increases with sintering temperature, T_{sint}, in the whole range of T_{sint}. The increase in ϵ' correlates with an increase in ceramic density as shown in Fig. 3. In the case of the BMT and BZN samples, however, ϵ' initially increases until it reaches a maximum of 24 and 40 for a sintering temperature of 1650 and 1440 °C, respectively. At a higher T_{sint}, the dielectric constant of BMT and BZN samples slightly decreases. The maximum values of ϵ' at 10 GHz obtained for BMT, BMN,

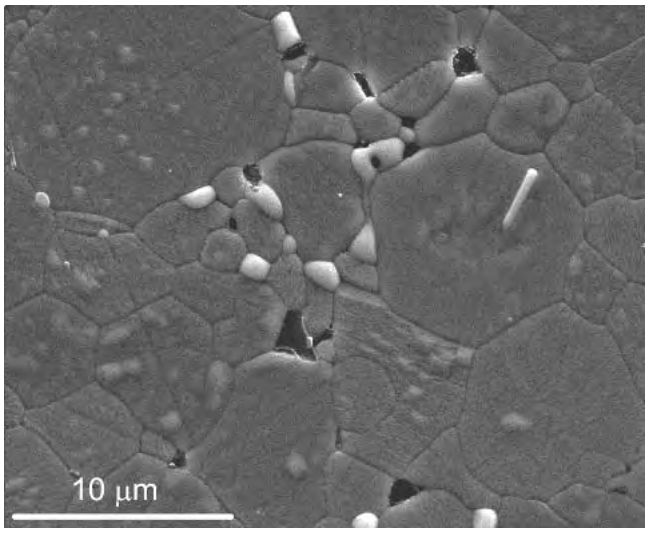

FIG. 5. SEM image of BMT sample sintered at 1700 °C. The second phase, having a light-gray color, is formed in the intergranular regions and on the surface of the matrix grains.

BNT, BNN, and BZN were 24, 31.4, 21.5, 35.4, and 40, respectively. These values are in a good agreement with those reported in the literature (Table I).

Figure 7 demonstrates the dependence of $Q \times f$ on the sintering temperature for BMT, BMN, BNT, BNN, and BZN ceramics. It is evident from Fig. 7 that the dielectric loss of the samples studied is very sensitive to the sintering temperature. Except for the BNT system, the $Q \times f$ exhibits a maximum as a function of T_{sint}. The decrease of $Q \times f$ following the maximum is especially pronounced in the BMT, BMN, and BNN samples. For BMT, the decrease of $Q \times f$ can be partially explained by the decrease in 1:2 cation ordering, which is observed for samples sintered above 1600 °C (Fig. 2). It is interesting, however, that for BMN and BNN the decrease of $Q \times f$ at high sintering temperatures cannot be explained by the intrinsic dielectric loss (i.e., decrease in the ordering parameter), since, according to Fig. 2, both BMN and BNN remained perfectly ordered up to 1620 and 1500 °C, respectively. Hence, an extrinsic source is responsible for the decrease in $Q \times f$. Extrinsic dielectric loss may originate from point defects, porosity, second phase, or grain boundaries. In our case, the significant drop in $Q \times f$ cannot be attributed to increase in porosity, since ceramics sintered at the highest temperatures still possess a relative density of 95–98% as shown in Fig. 3. Hence, one may conclude that the major source of the decay in $Q \times f$ is the formation of the second phase with high dielectric loss. Indeed, XRD analysis has detected $Ba_3Nb_5O_{15}$ second phase in both BMN and BNN sintered at 1620 and 1400 °C, respectively. This phase is a structural analog of the $Ba_3Ta_5O_{15}$ phase observed in BMT sintered above 1630 °C.

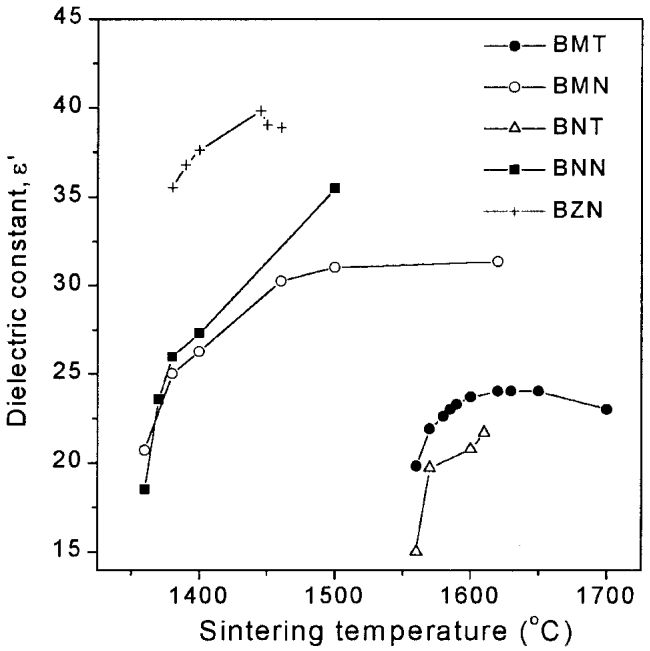

FIG. 6. Effect of sintering temperature on dielectric constant of BMT, BMN, BNT, BNN, and BZN ceramics.

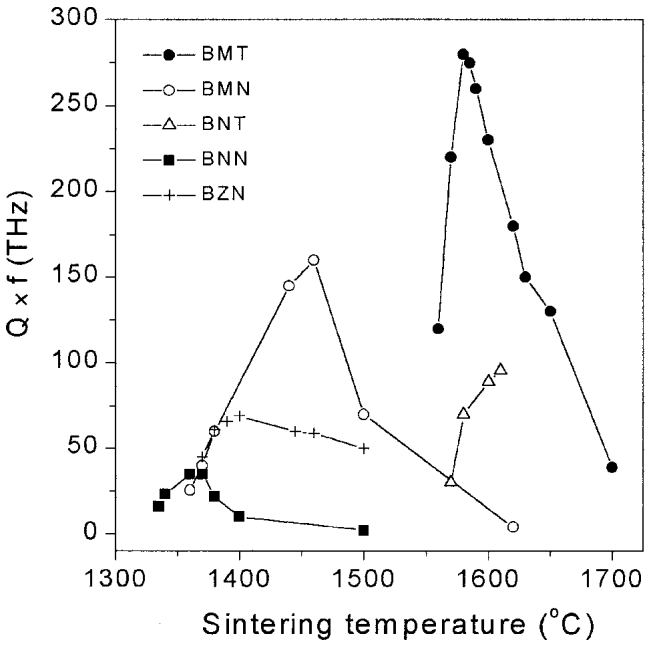

FIG. 7. Effect of sintering temperature on $Q \times f$ of BMT, BMN, BNT, BNN, and BZN dielectric resonators.

Similar to BMT, BMN, and BNN, formation of a second phase was observed in BZN ceramics sintered above 1440 °C. The crystallographic structure of this phase was different from $Ba_3Nb_5O_{15}$, but it was not possible to identify this phase using the JCPDS database. However, since the $Q \times f$ of BZN did not decrease significantly at high T_{sint}, it could be concluded that the unidentified second phase had relatively low dielectric loss. It should also be emphasized that all BZN samples analyzed at 10 GHz were disordered. This may partially explain the lower values of $Q \times f$ compared to the literature data summarized in Table I. The BNT sample showed a sharp increase of $Q \times f$ with sintering temperature. This is mainly attributed to the elimination of porosity in BNT ceramics and an increase in the ordering parameter as demonstrated in Figs. 2 and 3. The XRD analysis did not reveal any second phase in BNT sintered at 1000–1610 °C.

Measurements of the temperature coefficient of the resonance frequency, τ_f, of BMT, BMN, BZN, BNN, and BNT dielectric resonators were performed at 20 to 90 °C by using a rectangular copper waveguide. Using the test dielectric resonator, the waveguide contribution to the τ_f was found to be -1.2 ± 0.5 ppm/K. Figure 8 shows the effect of sintering temperature on τ_f. In the case of BMN, $\tau_f = +14 \pm 1$ ppm/K at $T_{sint} < 1470$ °C. At higher sintering temperatures, τ_f increases, reaching $+33.9 \pm 1$ ppm/K at $T_{sint} = 1620$ °C. A very important finding is that the τ_f of BNN obtained in this study differs significantly from

that reported in the literature (e.g., $\tau_f = +20$ ppm/K).[16] As shown in Fig. 8, the value of τ_f of BNN increases from −4.9 ppm/K at $T_{sint} = 1360$ °C to +5 ppm/K at $T_{sint} = 1500$ °C. The relatively high value of ϵ' and the nearly zero value of τ_f make BNN a promising compound for technical application. However, more work is required to improve its *Q* factor. The temperature coefficient of the resonance frequency of BZN varied in the range of +20.7 to +23 ppm/K. The BNT sample showed a decrease of τ_f with increasing sintering temperature from −10.5 to −13.5 ppm/K. The most significant effect of T_{sint} on τ_f was observed for BMN and BNN compounds. It is most likely that this effect is associated with an increase in the volume of residual $Ba_3Nb_5O_{15}$ in the samples. This phase apparently has a negative temperature coefficient of the dielectric constant which causes an increase in the τ_f of BMN and BNN resonators.

E. EPR analysis

Another contribution to dielectric loss arises from point defects (e.g., impurities, vacancies, interstitials). Interaction of these defects with electromagnetic field will result in absorption of part of the electromagnetic energy which otherwise would be stored in the resonator. Unfortunately, little is known about the point defect chemistry of $Ba(B'_{1/3}B''_{2/3})O_3$ compounds. Lee *et al.*[40] found that substitution of K for Ba in $Ba(Zn_{1/3}Ta_{2/3})O_3$ resulted in a decrease of 1:2 cation ordering. However, substitution of La for Ba resulted in a 1:2 to 1:1 phase transformation.[40] It can be assumed that A-site acceptor impurities in $Ba(B'_{1/3}B''_{2/3})O_3$ are compensated by oxygen vacancies or by an increase of the oxidation state of the B′ transition metal ions. Some of the point defects having unpaired electron spin can be detected using the EPR technique. Figure 9 demonstrates the room-temperature EPR spectra of BMT, BMN, BNN, BZN, and BNT dielectrics showing characteristic resonance peaks originating from the paramagnetic centers. As revealed by Fig. 9, the giromagnetic constant, *g*, of the major EPR peaks of the BMT, BMN, and BZN samples are very close to that of the unbound electron (i.e., $g_e = 2.0023$). These EPR signals may originate either from extrinsic defects such as Fe^{3+} and Cr^{3+} impurities or from intrinsic point defect with a captured hole.[41] Apparently, holes in these perovskites compensate for the accidental acceptor impurities, or negatively charged cation vacancies. The BNT compound shows two EPR singlets with $g = 2.510$ and 2.001. BNN compound shows a weak signal at $g = 2.003$ superimposed on a very broad EPR signal. This broad EPR signal may originate from the Ni ions having different oxidation states. The coexistence of Ni^{2+} and Ni^{3+} ions in Ni doped $Ba(Zn_{1/3}Ta_{2/3})O_3$ was recently discussed by Rong *el al.*[6] However, a detailed study of the point defect chemistry of $Ba(B'_{1/3}B''_{2/3})O_3$ perovskites is required to unambiguously identify the EPR signals presented in Fig. 9. At this point it is important to emphasize that the perovskites studied in this work are not free from point defects which contribute to the extrinsic dielectric loss. A more detailed study of point defects by EPR and positron annihilation techniques is currently under way in our laboratory.

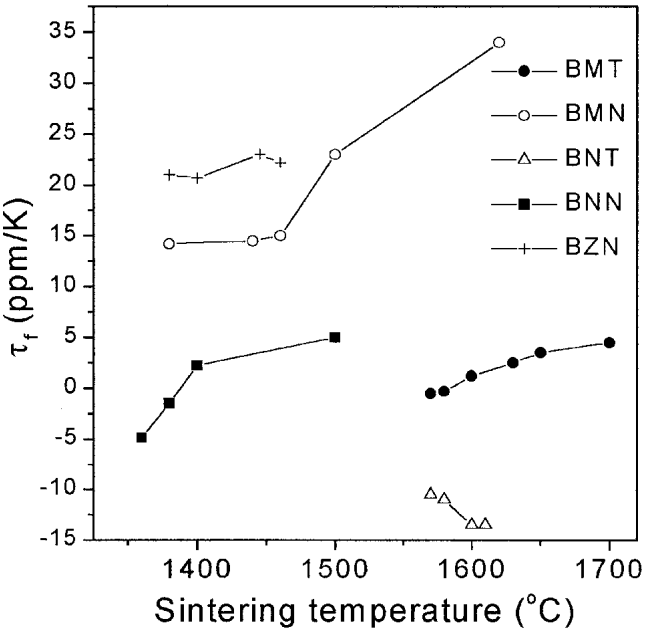

FIG. 8. Effect of sintering temperature on τ_f of BMT, BMN, BNT, BNN, and BZN dielectric resonators.

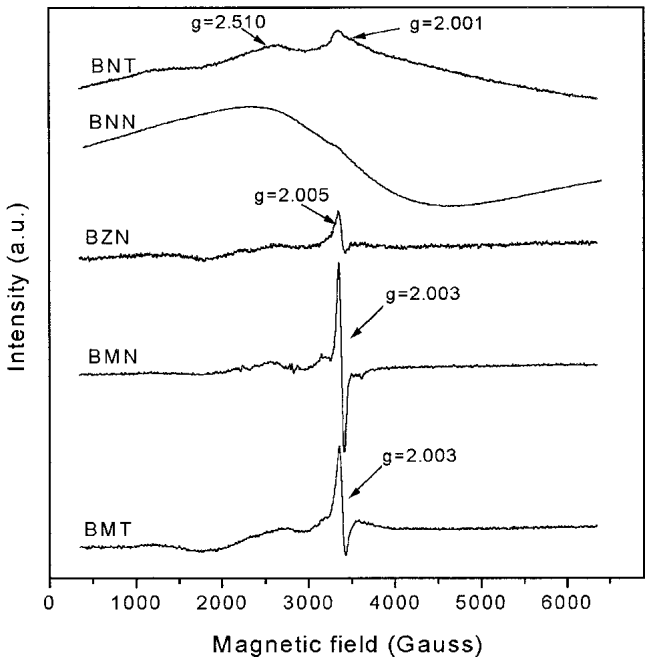

FIG. 9. Room-temperature electron paramagnetic resonance spectra of BMT, BMN, BNT, BNN, and BZN.

IV. CONCLUSIONS

In conclusion, the effect of preparation conditions on B-site cation ordering and dielectric properties of BMT, BMN, BZN, BNN, and BNT complex perovskites was investigated. It was found that all studied perovskites attained a high degree of 1:2 ordering at temperatures specific for each composition. A high-temperature order–disorder phase transition in BZN occurred below 1380 °C in agreement with the results of Hong *et al.*[15] However, coarse-grained BNN remained well ordered at temperatures as high as 1500 °C in contrast to the report of Hong *et al.*[23] One of the most important results is that the second phase ($Ba_3Ta_5O_{15}$, $Ba_3Nb_5O_{15}$) formed at high sintering temperatures (i.e., T_{sint} > 1400–1500 °C) plays a major role in the decrease in *Q* factor of BMT, BMN, and BNN samples. An increase in τ_f of the BMT, BMN, and BNN resonators may also be attributed to the increasing amount of the second phase at high sintering temperatures. It was also revealed by EPR that all samples studied contain a substantial amount of point defects. These defects contribute to the extrinsic dielectric loss at microwave frequencies,[5] thus degrading the *Q* factor. The chemical nature and precise identification of these defects requires further investigation.

ACKNOWLEDGMENT

We wish to acknowledge the Natural Sciences and Engineering Council of Canada for financial support.

REFERENCES

1. *Ceramic Transaction: Materials and Processes for Wireless Communication*, edited by T. Negas and H. Ling (American Ceramic Society Publications, Westerville, OH, 1995), Vol. 53.
2. N. Klein, A. Scholen, N. Tellmann, C. Zuccaro, and K.W. Urban, IEEE Trans. Microwave Theory Tech. **44,** 1369 (1996).
3. P.K. Davies, J. Tong, and T. Negas, J. Am. Ceram. Soc. **80,** 1727 (1997).
4. H. Matsumoto, H. Tamura, and K. Wakino, Jpn. J. Appl. Phys. **30,** 2347 (1991).
5. J. Petzelt and N. Setter, Ferroelectrics **150,** 89 (1993).
6. G. Rong, N. Newman, B. Shaw, and D. Cronin, J. Mater. Res. **14,** 4011 (1999).
7. V.L. Gurevich and A.K. Tagantsev, Adv. Phys. **40,** 719 (1991).
8. S-H. Ra and P.P. Phule, J. Mater. Res. **14,** 4259 (1999).
9. Y. Fang, A. Hu, S. Ouyang, and J. Oh, J. Eur. Ceram. Soc. **21,** 2745 (2001).
10. MuRata Electronics North America, RF and Microwave Products Catalog (1996).
11. S. Nomura, Ferroelectrics **49,** 61 (1983).
12. M.A. Akbas and P.K. Davies, J. Am. Ceram. Soc. **81,** 670 (1998).
13. H.J. Lee, H.M. Park, Y.K. Cho, H. Ryu, J.H. Paik, S. Nahm, and J.D. Byun, J. Am. Ceram. Soc. **83,** 937 (2000).
14. H.J. Lee, H.M. Park, Y.W. Song, and Y.K. Cho, J. Am. Ceram. Soc. **84,** 2105 (2001).
15. H. Tamura, T. Konoike, Y. Sakabe, and K. Wakino, J. Am. Ceram. Soc. **67,** 59 (1984).
16. H. Banno, F. Mizuno, T. Takeuchi, T. Tsunooka, and K. Ohya, *Proceedings of the 5th Meeting on Ferroelectric Materials and Their Applications* (Jpn. J. Appl. Phys. **21,** Supplement 24-3, 1985), p. 87.
17. M. Onoda, J. Kuwata, K. Kaneta, K. Toyama, and S. Nomura, Jpn. J. Appl. Phys. **21,** 1707 (1982).
18. F. Galasso and J. Pyle, J. Phys. Chem. **67,** 1561 (1963).
19. T. Hiuga and K. Matsumoto, Jpn. J. Appl. Phys. **28,** 56 (1989).
20. D.J. Barber, K.M. Moulding, J. Zhou, and M.Q. Li, J. Mater. Sci. **32,** 1531 (1997).
21. H. Yoshioka, Bull. Chem. Soc. Jpn. **60,** 3433 (1987).
22. M.A. Akbas and P.K. Davies, J. Am. Ceram. Soc. **81,** 1061 (1998).
23. K.S. Hong, I-T. Kim, and C-D. Kim, J. Am. Ceram. Soc. **79,** 3218 (1996).
24. I. Molodetsky and P.K. Davies, J. Eur. Ceram. Soc. **21,** 2587 (2001).
25. J. Venkatesh, V. Sivasubramanian, V. Subramanian, and V.R.K. Murthy, Mater. Res. Bull. **35,** 1325 (2000).
26. I. Qazi, I.M. Reaney, and W.E. Lee, J. Eur. Ceram. Soc. **21,** 2613 (2001).
27. T. Takahashi, E.J. Wu, and G. Ceder, J. Mater. Res. **15,** 2061 (2000).
28. T. Takahashi, Jpn. J. Appl. Phys. **39,** 5637 (2000).
29. T.V. Kolodiazhnyi, A. Petric, G.P. Johari, and A.G. Belous, J. Eur. Ceram. Soc. **22,** 2013 (2002).
30. D. Kajfez and P. Guillon, *Dielectric Resonators* (Artech Hause, Dedham, MA, 1986).
31. X.M. Chen, Y. Suzuki, and N. Sato, J. Mater. Sci., Mater. Electron. **5,** 244 (1994).
32. H-J. Youn, K-Y. Kim, and H. Kim, Jpn. J. Appl. Phys. **35,** 3947 (1996).
33. C.R. Feger and R.P. Ziebarth, Chem. Mater. **7,** 373 (1995).
34. B. Hessen, S.A. Sunshine, T. Siegrist, A.T. Fiory, and J.V. Waszczak, Chem. Mater. **3,** 528 (1991).
35. S. Nomura, K. Toyama, and K. Kaneta, Jpn. J. Appl. Phys. **21,** L624 (1982).
36. K. Matsumoto, T. Hiuga, K. Takada, and H. Ichimura, *6th IEEE International Symposium on Applications of Ferroelectrics* (IEEE, Piscataway, NJ, 1986), p. 118.
37. S.B. Desu and H.M. O'Bryan, J. Am. Ceram. Soc. **68,** 546 (1985).
38. S. Kawashima, N. Nishada, I. Ueda, and H. Ouchi, J. Am. Ceram. Soc. **66,** 421 (1983).
39. F.S. Galasso, *Structure, Properties and Preparation of Perovskite-Type Compounds* (Pergamon Press, Oxford, U.K., 1969).
40. C-C. Lee, C-C. Chou, and D-S. Tsai, J. Am. Ceram. Soc. **80,** 2885 (1997).
41. J. Bartoll (private communication).